

# Time-Resolved ESR Examination of a Simple Supramolecular Guest-Host System. Electron Spin Exchange Interaction in Micellized Spin-Correlated Radical Pairs

Chung-Hsi Wu, William S. Jenks,<sup>†</sup> Igor V. Koptuyug,<sup>‡</sup> Naresh D. Ghatlia, Matthew Lipson, Valery F. Tarasov, and Nicholas J. Turro\*

Contribution from the Department of Chemistry, Columbia University, New York, New York 10027

Received June 9, 1993\*

**Abstract:** The electron spin exchange interaction between micellized spin-correlated radical pairs (SCRPs) is investigated by time-resolved electron spin resonance (TRESR) spectroscopy. On the basis of the SCRPs model proposed independently by Closs and McLauchlan, an effective exchange interaction ( $J_{\text{eff}}$ ) can be extracted either from a direct reading of the observed TRESR spectra or through spectral simulation. The results for a series of micellized radical pairs (of similar electronic and magnetic structure) show that the  $J$  values are a function of the effective micelle size ( $L_{\text{eff}}$ ) experienced by a given micellized radical pair and also a function of the radical pair molecular structure for a given micelle size. The values of  $J_{\text{eff}}$  can be systematically manipulated by varying the size of the micelles and/or the structure of the radical pairs. The results are shown to be consistent with a simple model of the structure of the micelle which includes the relationship between the magnitude of the exchange interaction between the fragments of the micellized radical pair and the micellar parameters such as the frequency of geminate pair reencounters, the relative diffusion coefficient of the fragments in the micelles, and the effective volume of the micelle explored by the pair during the time of observation. It is shown that a micellized radical pair, because of interactive spin and molecular dynamics, constitutes a simple and useful model of a guest-host supramolecular structure so that variations of the micelle size and the radical pair structure are interacting and not independent variables.

## Introduction

Reactive radical pairs, created by flash photolysis of appropriate precursors in homogeneous solution in the cavity of an electron spin resonance (ESR) spectrometer, often exhibit a non-Boltzmann electronic spin distribution when observed by time-resolved electron spin resonance (TRESR) techniques, i.e., the radicals exhibit spin polarization. This phenomenon has been generally termed chemically induced dynamic electron polarization (CIDEP), and several mechanisms that give rise to this phenomenon have been recently reviewed.<sup>1-3</sup> Two of the most important polarization mechanisms are the triplet mechanism (TM) and the radical pair mechanism (RPM),<sup>4,5</sup> which provide complementary information on the mechanism of radical pair reactions in the sense that TM polarization originates in the steps prior to geminate radical pair formation, while RPM arises in steps subsequent to geminate radical pair formation. Both mechanisms lead to CIDEP spectra that are readily distinguishable by examination of the hyperfine patterns: (1) TM results in a pattern of hyperfine lines which are entirely of the same phase, i.e., entirely emissive or entirely absorptive and (2) RPM results in a pattern of hyperfine lines showing opposite phases about the center field of the EPR spectrum, i.e., absorptive in low field and

emissive in high field (A/E) or emissive in low field and absorptive in high field (E/A). Which of these two possibilities is observed can be predicted by the use of a simple equation (1) suggested by Adrian.<sup>7</sup>

The sign of the hyperfine pattern generated by RPM (designated as an E/A or A/E) may be predicted through eq 1,<sup>6,7</sup>

$$\Gamma_{\text{ME}} = -\mu \text{sign}(J) \quad (1)$$

where the value of  $\mu$  is determined by the multiplicity of the immediate precursor to the radical pair (1 for the triplet state and -1 for the singlet state) and  $\text{sign}(J)$  is determined by the ground-state multiplicity of the radical pair (-1 for singlet ground states and 1 for triplet ground states). If  $\Gamma_{\text{ME}} > 0$ , the polarization is of the E/A type; otherwise, the polarization is of the A/E type. The majority of reported CIDEP spectra result from triplet precursors possessing singlet ground states so that the sign of  $\Gamma$ , according to eq 1, is (-)(+)(-) = +, i.e.,  $\Gamma > 0$  and an E/A pattern is predicted.

A third type of CIDEP pattern has been observed in which individual hyperfine lines exhibit both absorptive and emissive components.<sup>8-13</sup> This pattern was observed in TRESR experiments involving both biradicals<sup>14</sup> and micellized radical pairs.<sup>8-12</sup>

<sup>†</sup> Present address: Department of Chemistry, Iowa State University, Ames, IA 50010.

<sup>‡</sup> Permanent address: Institute of Chemical Kinetics and Combustion, Novosibirsk 630090, Russia.

\* Abstract published in *Advance ACS Abstracts*, October 1, 1993.

(1) Muus, L. T.; Atkins, P. W.; McLauchlan, K. A.; Pedersen, J. B. *Chemically Induced Magnetic Polarization*; Reidel: Dordrecht, Holland, 1977; Chapters V-IX, XI, XIX.

(2) McLauchlan, K. A. *Advances in Pulsed and Continuous-Wave Electron Spin Resonance*; Wiley: New York, 1990; for general reference.

(3) Salikhov, K. M.; Molin, Y. N.; Sagdeev, R. Z.; Buchachenko, A. L. *Spin Polarization and Magnetic Effects in Radical Reactions*; Elsevier: Amsterdam, 1984; Chapters 2, 4, 8.

(4) Jenks, W. S.; Turro, N. J. *Res. Chem. Intermed.* 1990, 13, 237.

(5) Wan, J. K. S.; Tse, M. Y.; Depew, M. C. *Res. Chem. Intermed.* 1992, 18, 227.

(6) Grant, A. I.; Green, N. J. B.; Hore, P. J.; McLauchlan, K. A. *Chem. Phys. Lett.* 1984, 110, 280.

(7) Adrian, F. J. *J. Chem. Phys.* 1972, 57, 5107.

(8) Sakaguchi, Y.; Hayashi, H.; Murai, H.; I'Haya, Y. *J. Chem. Phys. Lett.* 1984, 110, 275.

(9) Sakaguchi, Y.; Hayashi, H.; Murai, H.; I'Haya, Y. J.; Mochida, K. *Chem. Phys. Lett.* 1985, 120, 401.

(10) Murai, H.; Sakaguchi, Y.; Hayashi, H.; I'Haya, Y. *J. Phys. Chem.* 1986, 90, 113.

(11) Buckley, C. D.; Hunter, D. A.; Horp, P. J.; McLauchlan, K. A. *Chem. Phys. Lett.* 1987, 135, 307.

(12) Closs, G. L.; Forbes, M. D. E.; Norris, J. J. R. *J. Phys. Chem.* 1987, 91, 3592.

(13) Closs, G. L.; Forbes, M. D. E. *J. Am. Chem. Soc.* 1987, 109, 6185.

(14) Closs, G. L.; Forbes, M. D. E.; Piotrowiak, P. *J. Am. Chem. Soc.* 1992, 114, 3285.

The spin-correlated radical pair model (SCRPM) was proposed independently by Closs<sup>12</sup> and McLauchlan<sup>11</sup> to explain these observations. In the SCRPM, the electron exchange interaction<sup>6,15-17</sup>  $J$  is assumed to be a factor which may dominate and modulate the electron spin-spin interactions under the high magnetic field approximation, while the dipolar interaction between electron spins is either ignored or treated as a constant.<sup>11,12</sup> The emission/absorption pattern of each hyperfine line occurs due to a rapid  $S-T_0$  intersystem crossing induced by hyperfine interaction, which both drains the  $T_0$  state (leading to excess population of  $T_+$  and  $T_-$ ) and splits the energies of  $T_0$  and  $S$  (leading to a splitting of the energies of the  $T_+ \rightarrow T_0$  and  $T_- \rightarrow T_0$  transitions). The SCRPM is discussed in detail in the spectral simulation section of this paper.

One important outcome of the SCRPM is that the sign and magnitude of the exchange interaction  $J$  can be extracted either from a direct reading of the recorded TRESR spectra or through spectral simulation.<sup>11,12,14,18</sup> It is generally assumed that the magnitude of  $J$  is approximated by an exponentially decaying function of the distance between the radical centers.<sup>7,16,17,19</sup> However, as the time resolution of conventional (continuous wave) ESR spectrometers is longer (ca. 200 ns)<sup>20</sup> than the time required for the spatial equilibration of the micellized radical centers (ca. 10 ns),<sup>21</sup> the observed TRESR spectra for micellized radical pairs are the distance-averaged spectra for the radical centers, that is to say, the  $J$  values extracted from the spectra are actually the average of "effective"  $J$  values  $J_{\text{eff}}$  experienced by the radical centers during the time scale of the TRESR measurements. In general, the observed spectra will consist of a superimposition of the spectra of micellized geminate pairs, micellized random pairs, and radicals in the bulk aqueous phase.

Supramolecular chemistry has been defined as "chemistry beyond the molecule".<sup>22,23</sup> Guest-host complexes constitute an important class of supramolecular systems. Guest-host systems are related to molecules (and the noncovalent intermolecular bond) as molecules are related to atoms (and the covalent intramolecular bond), i.e., guest-host chemistry is concerned with the structure and dynamics of entities consisting of two or more molecules that are held together by noncovalent bonds. The guest is usually a small molecule which is noncovalently associated with (i.e., is bound to) a host, the latter entity often being a large single molecule or a self-assembling aggregate of molecules, such as micelles. To the extent that a guest-host complex is stoichiometric (or is close to stoichiometric) and may be viewed as operating as a unit during an observable process, we may consider such a complex as a sort of supermolecule.

If a micellized radical pair is considered as a prototypical guest-host complex, i.e., a supramolecular system, certain useful analogies may be drawn between "supramolecular" micellized radical pairs and "molecular" biradicals connected by a flexible methylene chain. Flexible biradicals exist in a distribution of conformations which are characterized by different separations  $r$  between the two radical centers. It is this equilibrium of conformations which determines the average distance of separation of the radical centers during the TRESR experiments. Micellized radical pairs, however, exist in a distribution of different sites

within the micelle and are in a dynamic state of exchange between these sites. Therefore, the distance-averaged TRESR spectra for micellized radical pairs reflect an effective micelle size (with a characteristic radius  $L_{\text{eff}}$ ) experienced by the radical pair fragments during the time scale of the TRESR experiments.

An important feature of supramolecular systems is that they possess observable properties that differ significantly from simple addition of the corresponding properties of the molecular analogues. In the case of micellized radical pairs, the analogous "molecular" system that we chose for comparison is a radical pair in a nonviscous homogeneous solution. For such radical pairs, the time for diffusional separation to  $10 \text{ \AA}$  ( $\sim 10^{-10} \text{ s}$ )<sup>24,25</sup> is usually fast enough that, by the earliest time for TREP spectra to be recorded (ca. 200 ns after the ca. 4-ns laser flash in our study), the effective  $J$  value between the fragments of the radical pair has dropped to zero. Furthermore, by this time, all the pairs have lost their geminate character and have achieved random positions in the solvent. However, for supramolecular micellized radical pairs, the micelle behaves as a "supercage"<sup>26</sup> compared to the solvent cage provided by the molecules of a homogeneous solvent. The micellar supercage may increase the time scale over which the geminate character of the radical pair fragments is preserved for orders of magnitude and may force the pair to remain spatially proximate for time periods of the order of  $10^{-6} \text{ s}$ .<sup>27</sup> Therefore, on time scales shorter than  $1 \mu\text{s}$ , a supramolecular micellized radical pair possesses constraints on spatial separation of the radical centers which are analogous to those of a molecular biradical.

The radical precursors chosen for this study are ketones 1-9 K listed in Chart I. Upon photolysis in homogeneous solution, all of these ketones undergo ultrafast intersystem crossing to the triplet state and very fast ( $>10^9 \text{ s}^{-1}$ ) Norrish type I reaction<sup>28</sup> which produces triplet radical pairs 1-9 RP (Chart I). The TRESR spectra of these radicals in homogeneous solution display emissive CIDEP spectra characteristic of TM polarization. In nonviscous homogeneous solvents, these CIDEP spectra, except for intensities, are not significantly influenced by the solvent nor the structure of the radicals generated by photolysis. On the other hand, the TRESR spectra of the same radicals in micellar solutions show CIDEP spectra, which are very dependent on the size of the micelle employed in generating the micelle and on the structure of the radicals produced by photolysis. The size variation in the micelles was achieved by changing the chain length of the surfactant monomers as well as by the addition of external electrolytes. Two kinds of surfactants, positively charged alkyl-trimethylammonium salts and negatively charged alkyl sulfate salts, were used in our studies.

The ketones investigated may be conveniently divided in two structural families, 1-6 K and 7-9 K, based on functional group considerations. Each family contains ketones which will produce radical pairs that are electronically and magnetically very similar and which differ mainly in alkyl substitution at sites remote from the radical centers. Our motivation in employing TRESR to investigate such a series of radical pairs is to vary systematically the distribution of the different sites occupied by the radical pair within a micelle by varying the structure of the individual fragments, and to study the influence of these variations on the values of  $J_{\text{eff}}$  obtained from the TRESR spectra (for those pairs displaying SCR behavior). In supramolecular terms, we are exploring the variation of supramolecular structure, i.e., the average "binding" of the radical pair to various sites of the micelle, the "conformational" dynamics which occur as the radical pair explores the possible sites within the micelle, and the "dissociation"

(15) Adrian, F. J. *J. Chem. Phys.* **1988**, *88*, 3216.

(16) Syage, J. A. *J. Chem. Phys.* **1987**, *87*, 1033.

(17) Syage, J. A. *J. Chem. Phys.* **1987**, *87*, 1022.

(18) Closs, G. L.; Forbes, M. D. E. *J. Phys. Chem.* **1991**, *95*, 1924.

(19) Kanter, F. J. J. D.; Hollander, J. A. D.; Huizer, A. H.; Kaptein, R. *Mol. Phys.* **1977**, *34*, 857-874.

(20) The typical loaded  $Q$  values for the TE102 mode cavities (as used at Columbia) are a few thousand, implying response times of ca. 150-250 ns for the micellar solution experiments in our studies.

(21) This is the approximate time required for the first visit of the radical pair fragments to the boundary of the micelle during a random walk. See: Tarasov, V. F.; Ghatlia, N. D.; Buchachenko, A. L.; Turro, N. J. *J. Am. Chem. Soc.* **1992**, *114*, 9517.

(22) Balzani, V.; Scandola, F. *Supramolecular Photochemistry*; Prentice-Hall: New York, 1991; Chapter 3.

(23) Lehn, J.-M. *Angew. Chem., Int. Ed. Engl.* **1988**, *27*, 89.

(24) Turro, N. J.; Weed, G. C. *J. Am. Chem. Soc.* **1983**, *105*, 1861.

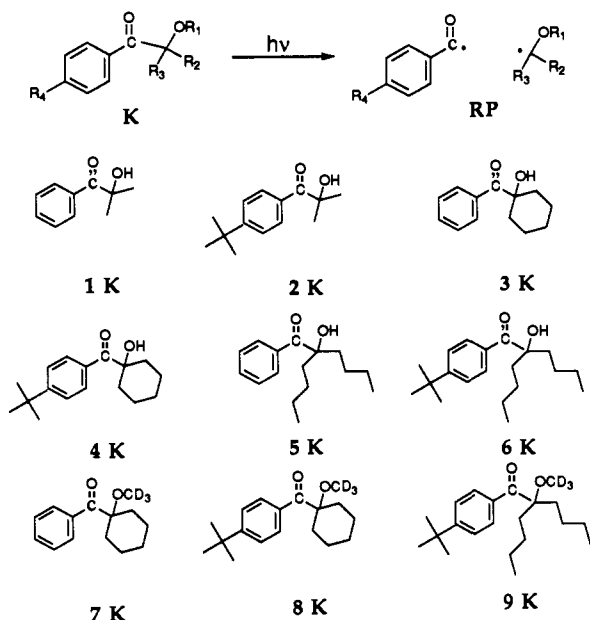
(25) Benson, S. W. *The Fundamentals of Chemical Kinetics*; McGraw Hill: New York, 1960; p 493.

(26) Turro, N. J.; Cherry, W. R. *J. Am. Chem. Soc.* **1978**, *100*, 7431.

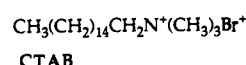
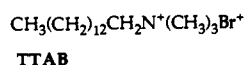
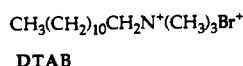
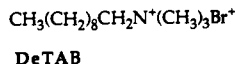
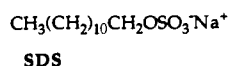
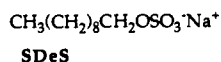
(27) Turro, N. J.; Zimmt, M. B.; Gould, I. R. *J. Am. Chem. Soc.* **1983**, *105*, 6347.

(28) Bamford, C. H.; Norrish, R. G. W. *J. Chem. Soc.* **1945**, 1504.

Chart I



## B) The surfactants



of the supramolecular structure when a radical fragment escapes into the bulk aqueous phase. If micellized radical pairs are viewed as supramolecular systems,<sup>22,23</sup> the results are not expected to be understood only on the basis of the guest radical pair structure (which is sufficient for measurements in nonviscous homogeneous solvents) but must also be considered in terms of the host micelle structure. Indeed, we shall show that both the radical pair structure and the micelle structure must be considered as interactive, in the sense of a true supramolecular system, in order to understand qualitatively and quantitatively and to interpret the results. For example, from the TRESR spectra observed, it will be shown that the relative escape rates of the radical fragments from the micelle supercages will depend both on the structure of the micelle and on the structure of the pair.

## Experimental Section

All ESR spectra were acquired on a Bruker ER100 D X-band ESR spectrometer operated in the direct detection mode with the signal acquired by an EG&G PARC 4402 boxcar and a 4422 integrator. The samples flowed through a flat cell with an optical path length of 0.5 mm at a rate of ca. 0.7 mL/min. Excitation was provided by a Quanta Ray DCR 2A Nd:Yag laser operating at 266 nm and 20 Hz with a pulse of ca. 4 ns fwhm. The pulse energy was controlled at  $15 \pm 1$  mJ/pulse.

Phenyl 1-hydroxycyclohexyl ketone (3 K, Ciba-Geigy), manganese chloride tetrahydrate ( $\text{MnCl}_2 \cdot 4\text{H}_2\text{O}$ , Sigma), dodecyltrimethylammonium

bromide (DeTAB, Kodak), dodecyltrimethylammonium bromide (DTAB, Aldrich), tetradecyltrimethylammonium bromide (TTAB, Sigma), hexadecyltrimethylammonium bromide (CTAB, Sigma), sodium decyl sulfate (SDeS, Lancaster), and sodium dodecyl sulfate (SDS, Bio-Rad) were used as received. Potassium hexacyanochromate ( $\text{K}_3\text{Cr}(\text{CN})_6$ )<sup>29</sup> and ketones 1, 6, 7 K, and 9 K,<sup>30</sup> were synthesized according to published procedures. Ketones 2, 4, 5 K, and 8 K were synthesized in a manner analogous to that described for ketones 1, 6, 7 K, and 9 K. All the synthesized compounds were purified by flash column chromatography and satisfactorily characterized by GC-MS and <sup>1</sup>H- and <sup>13</sup>C-NMR spectroscopy.

Detergent solutions were prepared in deionized water. Concentration of the micelles was fixed at 1 mM for all the detergents used and was calculated according to the formula

$$[M] = ([S] - \text{cmc})/N$$

where [M] and [S] correspond to the concentration of micelle and surfactant, respectively, cmc is the critical micelle concentration,<sup>31,32</sup> and *N* is the aggregation number of the surfactant monomers. The concentration of radical pair precursors was 1.5 mM in most detergent solutions except 8 K was 1 mM in DeTAB ( $\text{C}_{10}^+$ ), 6 K was 1 mM in both DeTAB ( $\text{C}_{10}^+$ ) and SDS ( $\text{C}_{12}^-$ ), and 9 K was less than 0.5 mM in DeTAB ( $\text{C}_{10}^+$ ). The lower concentrations for the later systems were mandated by solubility considerations. The concentrations of the paramagnetic species  $\text{Mn}^{2+}$  and  $\text{Cr}(\text{CN})_6^{3-}$ , employed as polarization quenchers, were fixed at 5 mM.

Immediately prior to TRESR measurements, all samples were prepared by extended stirring of the radical precursors in micellar solutions with Ar bubbling to achieve deoxygenation.

## RESULTS

**TRESR Spectra for Homogeneous Solutions vs Micellar Solutions.** Figure 1a shows the TRESR spectrum obtained upon photolysis of 6 K in a homogenous solution composed of a mixture of *tert*-butyl alcohol and water (1:1), and Figure 1b shows the spectrum obtained from photolysis of 6 K in SDS micellar solution. Both spectra were acquired at 450 ns after the laser flash, and the gate width of the boxcar was 50 ns. The striking difference distinguishing these two spectra is that while Figure 1a shows a virtually entire emissive spectrum in which the signals from the benzoyl radical (an apparent singlet which displays fine structure at higher resolution, labeled with \* in the figures) and a ketyl radical (quintet) are clearly resolved, the spectrum in Figure 1b shows an emissive-absorptive (EA) pattern for each hyperfine line. This EA pattern is analogous to that reported by Closs et al. for the radical pair derived by photoreduction of benzophenone in SDS micelles and assigned to an SCRPs.<sup>12</sup> This pattern (Chart II) was interpreted in terms of a fast intersystem crossing (ISC) induced by hyperfine interactions (HFI) which occur under the influence of a weak electron spin exchange (ESE) interaction. According to Chart II, the maximum and minimum of each hyperfine line in Figure 1b are separated by  $2J_{\text{eff}}$ ,<sup>11,12</sup> where  $J_{\text{eff}}$  is an effective exchange interaction averaged over all locations of the radical pair fragments within the micelle. Thus, a qualitative estimate for the magnitude of the ESE may be obtained by directly measuring the value of  $2J_{\text{eff}}$  from the experimental spectra.

In nonviscous homogeneous solutions, the EA pattern is not seen in the CIDEP spectra (Figure 1a) of radical pairs because of a very fast loss of correlation (ca. 100 ps) due to diffusional separation of the pair;<sup>33-35</sup> in this case, the effective spin correlation

(29) Kruser, F. V. D.; Miller, E. H. *J. Am. Chem. Soc.* **1906**, *28*, 1133.

(30) Jenks, W. S. Ph.D. Thesis, Columbia University, 1991.

(31) Bunton, C. A.; Nome, F.; Quina, F. H.; Romsted, L. S. *Acc. Chem. Res.* **1991**, *24*, 357.

(32) Tanford, C. *The Hydrophobic Effect*; Wiley: New York, 1973; Chapter 7.

(33) Lazar, M.; Rychly, J.; Klimo, V.; Pelikan, P.; Valko, L. *Free Radicals in Chemistry and Biology*; CRC Press: Boca Raton, FL, 1989; p 13.

(34) Noyes, R. M. *J. Am. Chem. Soc.* **1956**, *78*, 5486.

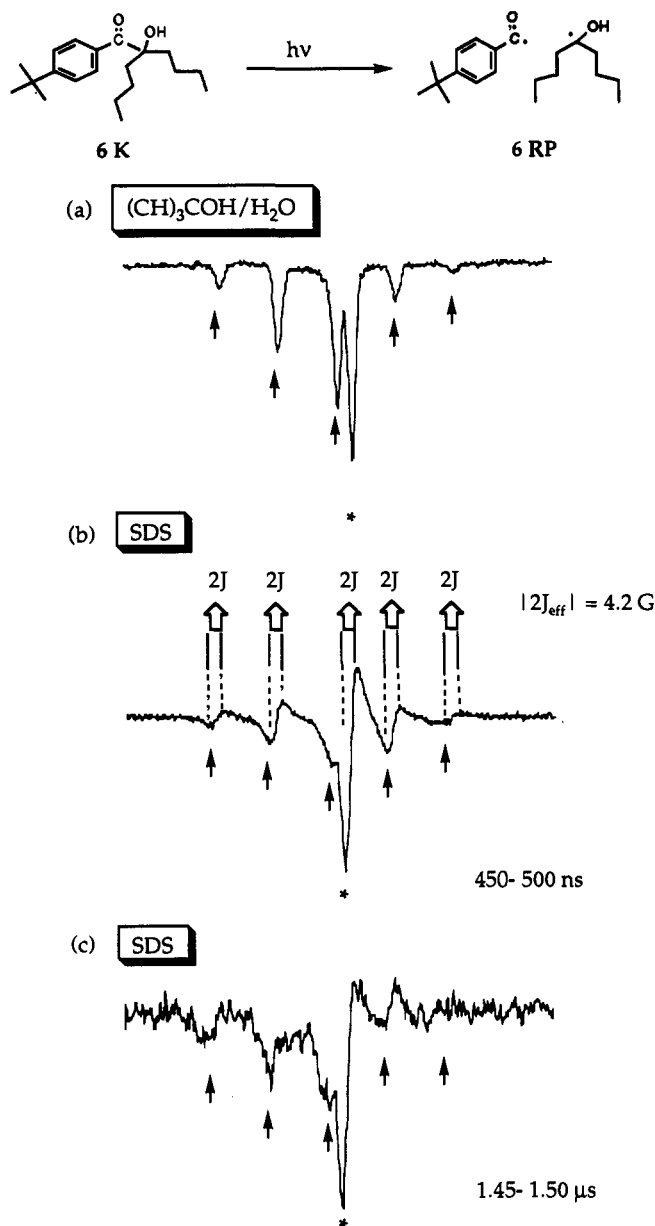


**Figure 1.** TRESR spectra observed during the photolysis of **6 K** in (a) a mixture of *tert*-butyl alcohol and water (1:1) and (b) SDS ( $C_{12}$ ) micellar solution. Excitation was at 266 nm for all spectra reported in this paper, and the detection window was from 450 to 500 ns after the laser flash. Spectrum c was recorded in the same condition as (b) except the detection time window was from 1450 to 1500 ns. All spectra are 120-G wide. The line attributable to the benzoyl radical is marked with an asterisk; the other lines are attributable to the ketyl radical and are marked with arrows.

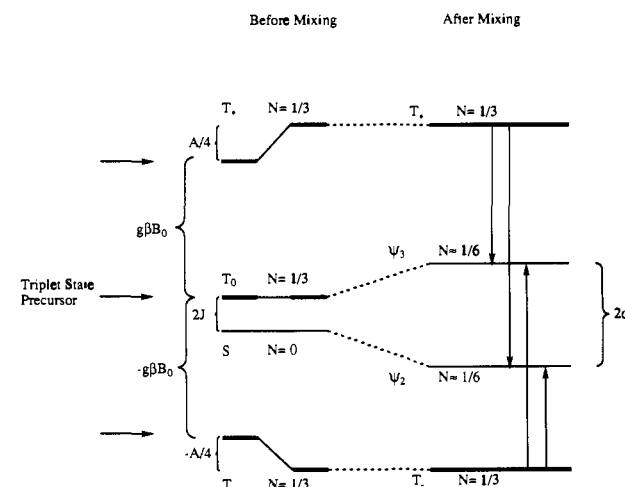
only lasts as long as the primary solvent cage<sup>34,36</sup> which is at least 2 orders of magnitude shorter lived than the earliest recorded TRESR spectra (150–250 ns). Careful inspection of Figure 1a shows that the emissive quintet of the  $\alpha$ -hydroxyalkyl radical is not completely symmetric; the intensities of the low-field emissive peaks are somewhat stronger than those of the high-field emissive peaks. This asymmetry is attributed to an E/A contribution of RPM in addition to a pure contribution of TM in the spectrum.<sup>3-5</sup>

In applying eq 1 to predict the phase of the expected RPM spectra,<sup>6,7</sup>  $\mu = 1$  since all the radical pairs investigated are generated from photoexcited ketones undergoing bond cleavage from excited triplet states. Furthermore, all radical pairs

(35) Kaptein, R. *Adv. Free-Radical Chem.* 1975, 5, 381.

(36) Rabinowitch, E.; Wood, W. *Trans. Faraday Soc.* 1936, 32, 1381.

**Chart II.** Energy-level Diagram of a Radical Pair in a Magnetic Field with One Hyperfine Interaction  $A$  and Exchange Interaction  $J^a$



<sup>a</sup> The left side of the figure shows zero-order levels, and the right side shows the levels after mixing. The initial population  $N$  is assumed to be in the triplet levels only.

generated have singlet ground states<sup>4,37</sup> (i. e.,  $J < 0$ ), and hence,  $\text{sign}(J) = -1$ . Therefore, if the RPM is operating to produce the observed polarization, we expect to see an E/A pattern in the EPR spectra since, for all cases investigated,  $\Gamma_{ME} > 0$ . When both TM and RPM contribute to a spectrum, the high-field absorptive peaks of RPM will somewhat offset the emissive peaks of TM at the same resonance frequency. At low fields, however, both RPM and TM give rise to emissive peaks and, hence, reinforce one another as observed in Figure 1a.

Since RPM polarization results from the spin evolution during diffusional dynamics, while TM and SCRPM polarization decay with increasing time,<sup>4,12</sup> it is expected that the contribution from intramolecular RPM to the recorded TRESR spectra at longer times will increase. This expectation is supported by comparing the spectra for micellized pair **6 RP** shown in Figures 1b and 1c, where the E/A pattern in Figure 1c shows that the RPM becomes the dominant mechanism in the TRESR spectrum recorded at longer times (1.45–1.50  $\mu\text{s}$ ).

**Effect of Micelle Size on the Value of  $J_{\text{eff}}$ .** Micellar size may be manipulated and varied systematically by changing the chain length of the surfactant monomer molecules that form the micelle or by adding external electrolytes. Both processes are known to influence the cmc and aggregation number of the micelle.<sup>32,38-40</sup> Figures 2a–d show the TRESR spectra obtained during the photolysis of **6 K** in alkyltrimethylammonium bromide micelles of systematically varying sizes ( $C_{10}^+ - C_{16}^+$ ) where  $C_n$  is the chain length of the surfactant monomer molecules and the superscript refers to the charge on the surfactant head group. The shape of the spectra and the absolute values of  $2J_{\text{eff}}$  (shown on the figure and summarized in Table IV), which are measured directly from the recorded spectra, clearly show a dependence on the alkyl chain length of the detergents:  $J_{\text{eff}}$  drops from 17.5 MHz (6.2 G) in DeTAB ( $C_{10}^+$ ) micelle to 7.8 MHz (2.8 G) in CTAB ( $C_{16}^+$ ) micelle. Qualitatively, it appears that the line widths decrease as the number of carbon atoms in the detergent monomer increases. In fact, the spectrum obtained in CTAB micelles ( $C_{16}^+$ , the largest monomer surfactant in the series) is almost purely emissive, as shown in Figure 2d, and shows little hint of an SCRPM contribution.

(37) Yankelovich, A. Z.; Potapov, V. K.; Hagemann, H. J.; Kuznets, V. K.; Pershin, A. D.; Buchachenko, A. L. *Bull. Acad. Sci. USSR* 1982, 31, 460.

(38) Chen, J.-M.; Su, T.-M.; Mou, C. Y. *J. Phys. Chem.* 1986, 90, 2418.

(39) Lei, X.-G.; Zhao, G.-H.; Liu, Y.-C.; Turro, N. J. *Langmuir* 1992, 8, 475.

(40) Aniansson, E. A. G.; Wall, S. N.; Almgren, M.; Hoffman, H.; Kielmann, I.; Ulbricht, W.; Zana, R.; Lang, J.; Tondre, C. *J. Phys. Chem.* 1976, 80, 905.

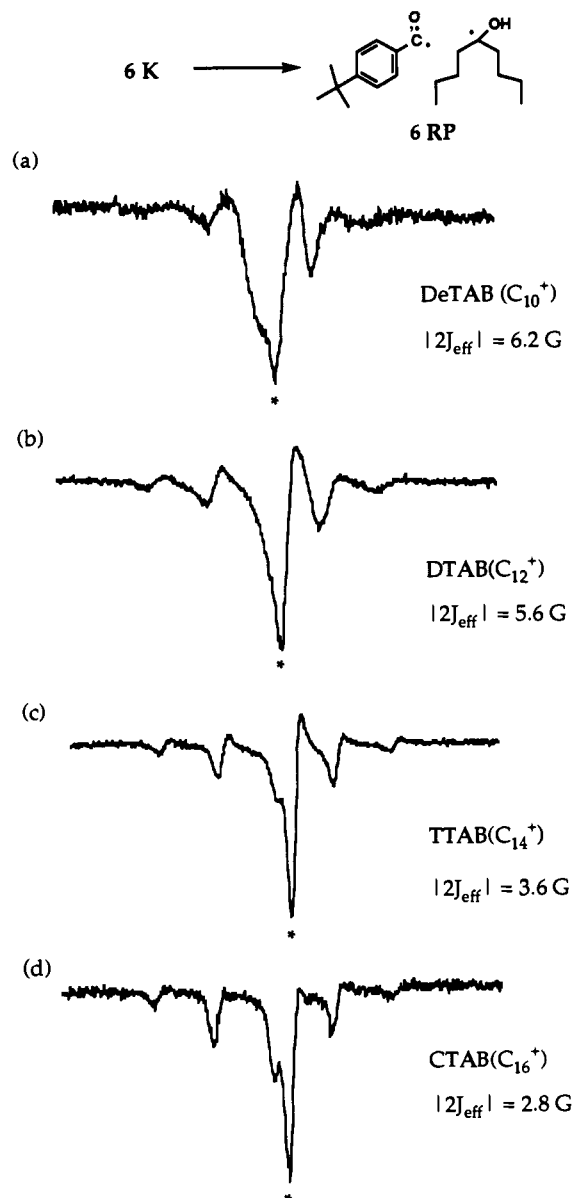


**Figure 2.** TRESR spectra obtained during photolysis of **6 K** in (a) DeTAB, (b) DTAB, (c) TTAB, and (d) CTAB micellar solutions. All spectra were recorded under the same sweep width (120 G) and detection time window (450–500 ns). The line attributable to the benzoyl radical is marked with an asterisk. The  $|2J_{\text{eff}}|$  values are measured directly from the spectra.

Analogous results are obtained in oppositely charged sodium alkyl sulfate micelles, in which the  $2J_{\text{eff}}$  values measured for the radical pair derived from **6 K** in  $C_{10}^-$  and  $C_{12}^-$  sulfates are 15.8 MHz (5.6 G) and 11.2 MHz (4.0 G), respectively.

A similar effect can be seen in the TRESR spectra obtained upon photolysis of **6 K** in SDS micellar solutions in the presence of increasing variable amounts (0–1 M) of added NaCl. The  $|2J_{\text{eff}}|$  value is 11.8 MHz (4.2 G) for **6 RP** in SDS micelle and then drops to 9.6 MHz (3.4 G), 9.0 MHz (3.2 G), and then 6.8 MHz (2.4 G) with the presence of 0.25, 0.5, and 1.0 M NaCl, respectively. Since the size of alkyl sulfate micelles increases as the external salt concentration increases,<sup>38,40–42</sup> these results are consistent with a systematic decrease in the  $J_{\text{eff}}$  values as the micelle size systematically increases.

**Effect of Radical Pair Structures on  $J_{\text{eff}}$ .** The above results demonstrate that the effectiveness of the exchange interaction

can be modulated by controlling the size of the micellar supercage. Since a micellized radical pair is a supramolecular structure, we anticipate that the structure of the guest radical pair, operating in conjunction with the structure of the host micelle, will also influence the value of  $J_{\text{eff}}$ . To examine the validity of this expectation, we have investigated a series of ketones which, when photolyzed, will produce radical pairs possessing very similar electronic and magnetic properties but which differ in their molecular structure by possessing different hydrophobic alkyl substituents at sites remote from the radical centers. These structural features are not expected to be of any significance in TRESR spectra obtained in homogeneous solutions because only uncorrelated radicals are observed experimentally. However, the sitings and dynamics of a radical pair in a micelle are supramolecular properties of the guest–host system and are therefore expected to depend on the structure of both moieties of the micellized radical pair. In terms of a crude model, the hydrophobicity (or the solubility) of each fragment of a micellized radical pair will depend on the number of carbon atoms of the fragment and of the surfactant making up the micelle and the hydrophobicity of the suprasiting.

Figures 3 and 4 show examples of the influence of variation of the radical pair structure on the ESE interaction in SDS micelles as deduced from TRESR. The values of  $2J_{\text{eff}}$ , measured as the separation of the adjacent emissive/absorptive peaks in the TRESR spectra, are presented in each spectrum in Figures 3 and 4. These spectra are obtained from the photolysis of micellized radical precursors **1–6 K** and **7–9 K**, which correspond to Figures 3a–f and 4a–c, respectively.

For radical pairs with similar electronic properties, magnetic properties, and polar groups, the number of carbon atoms is an approximate measure of the hydrophobicities of the corresponding radical pair fragments.<sup>32,43,44</sup> It is expected that the hydrophobic character of a radical pair will determine its solubility in a given micelle and that solubility will be a guide to the siting of the radical pair in the micelles and to the molecular dynamics of the radical pair, including the escape rates of the fragments of the pair from the micelles. Therefore, the results of Figures 3 and 4 are analyzed by investigating the relationship between the number of carbon atoms of each radical pair and the value of  $J_{\text{eff}}$  extracted from the TRESR spectra, as listed in Table I where the radical pairs are compared by holding the molecular structure of one radical fragment constant and by varying the structure of the other fragment. It can be seen (Table I) that the value of  $J_{\text{eff}}$  is a monotonic function of the number of carbon atoms in the variable fragment in a given series. For example, for the radical pairs **1 RP** and **2 RP**, both of which contain a small, hydrophilic three carbon ketyl fragment, the absolute value of  $2J_{\text{eff}}$  is nearly 0 (on the time scale of Figures 3a and 3b). Presumably, this is the result of the very low hydrophobicity of the ketyl fragment, which greatly reduces the residence time of the ketyl fragment in the micelle perhaps to a time shorter than the time scale of the experiment. However, the value of  $|2J_{\text{eff}}|$  increases to  $\sim 9.0$  MHz (3.2 G) for the radical pair **4 RP**, which contains two relatively hydrophobic fragments, one possessing 11 carbon atoms and the other 6 carbon atoms (Figure 3d). A further increase in  $|2J_{\text{eff}}|$  to 11.8 MHz (4.2 G) is observed for the radical pair **6 RP**, which contains two hydrophobic fragments containing 11 carbon atoms and 9 carbon atoms (Figure 3f).

Similar trends are found in the TRESR spectra shown in Figure 4. For the same micelle (SDS), the value of  $J_{\text{eff}}$  monotonically increases as the hydrophobicity within a family of the fragments increases. Employing the benzoyl–cyclohexyl pair in Figure 3 as a reference point, the value of  $|2J_{\text{eff}}|$  is too small to measure, i.e., less than 6.8 MHz (2.4 G). However, addition of one carbon atom to the cyclohexyl fragment increases  $|2J_{\text{eff}}|$  to a measurable

(41) Lianos, P.; Zana, R. *J. Phys. Chem.* **1980**, *84*, 3339.

(42) Turro, N. J.; Zimmt, M. B.; Lei, X. G.; Gould, I. R.; Nitsche, K. S.; Cha, Y. *J. Phys. Chem.* **1987**, *91*, 4544.

(43) Casal, H. L.; Martin, A. *Can. J. Chem.* **1989**, *67*, 1554.

(44) Ben-Naim, A. *Hydrophobic Interactions*; Plenum Press: New York, 1980; p 167.

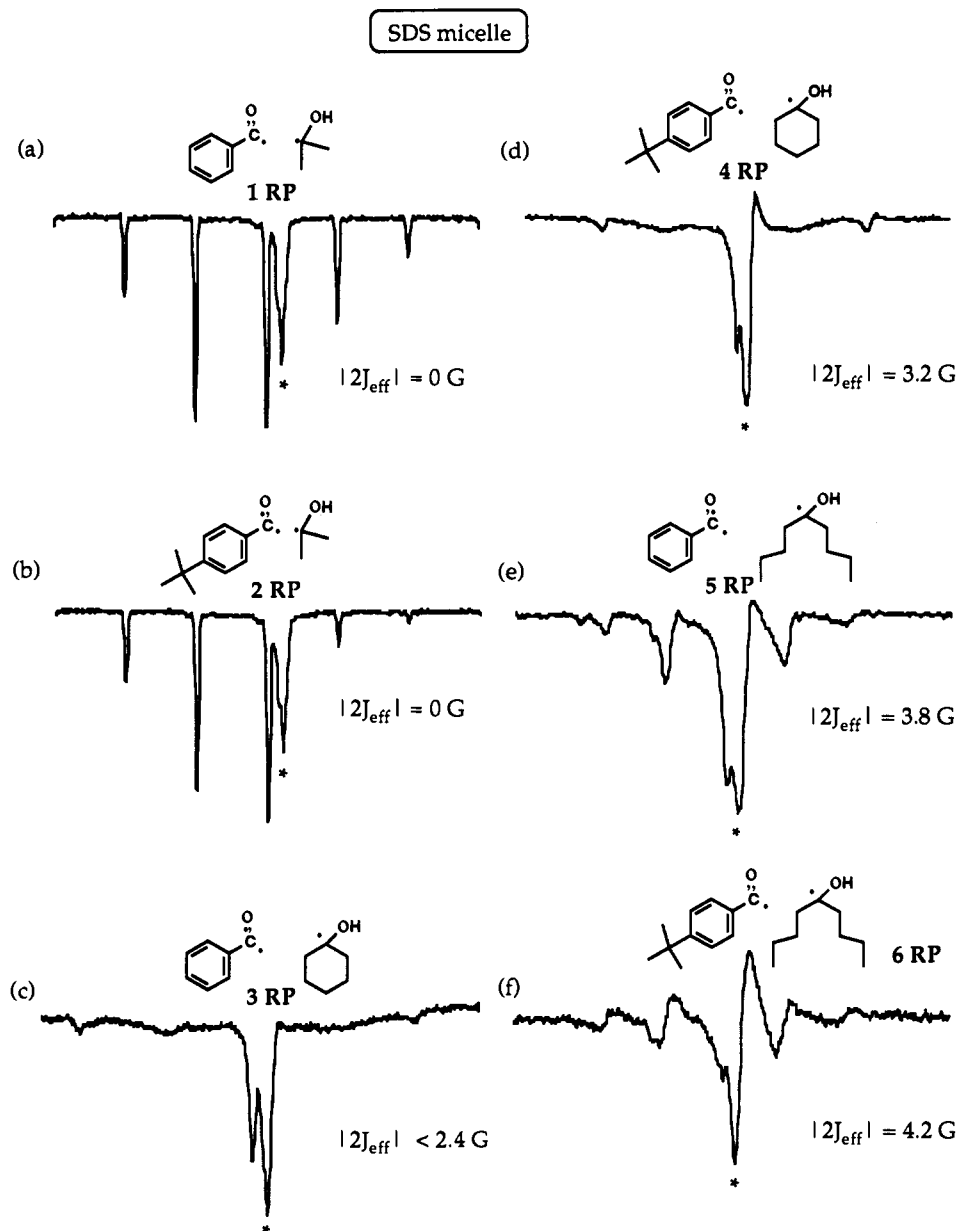


**Figure 3.** TRESR spectra of the radical pairs in SDS micellar solution recorded at 450–500 ns after the laser flash. All spectra are 120-G wide. Spectra a–f correspond to radical pairs derived from 1–6 K, respectively. The lines attributable to the benzoyl radicals are marked with asterisks, while the remainder of the lines are attributable to the ketyl radicals. The values of  $|2J_{\text{eff}}|$  in each spectrum are obtained directly from the spectra.

value of 3.0 G (Figure 4a), and attachment of an additional four-carbon group to the benzoyl fragment causes an increase in  $|2J_{\text{eff}}|$  to 3.8 G (Figure 4e). Confirming the trends, the radical pair 9 RP, which contains one more carbon atom than the radical pair 6 RP, possesses a larger value of  $|2J_{\text{eff}}|$  (5.2 G vs 4.2 G, respectively).

**Effect of Aqueous-Phase Paramagnetic Quenchers on the TRESR Spectra.** The TRESR spectra obtained in our investigations are expected to include not only signals from the correlated micellized radical pairs but also signals from the radicals which have exited the micelles and are in the bulk aqueous phase during the measurement and signals from the corresponding uncorrelated micellized radical pairs. The value of  $|2J_{\text{eff}}|$  for each spin-correlated micellized radical pair is conveniently determined as the separation between the emission/absorption peaks of each hyperfine line in the observed spectra. However, the superposition of the signals of the free radicals may shift the positions of the emission or absorption peaks of the correlated radical pair, resulting in an error when measuring the value of  $2J_{\text{eff}}$ . In order to diminish the contribution of radicals in the bulk aqueous phase to the observed spectra and to investigate the behavior of the TRESR spectra in

the presence of “polarization scavengers”, we studied the effect of introducing paramagnetic species carrying the same charge as the micellar head groups and functioning as aqueous-sited electron spin relaxants (polarization quenchers) of the radical fragments which escape from micelles and enter the bulk aqueous phase. Although stable nitroxides sequestered in the aqueous phase have been used to study the exit rates of radicals by acting as polarization acceptors,<sup>45</sup> the polarized signals of the nitroxide can overlap with and obscure the signals of the correlated micellized radical pairs. Therefore, quenchers such as  $\text{Mn}^{2+}$  or  $\text{Cr}(\text{CN})_6^{3-}$ , which do not contribute any ESR signal themselves to the observed TRESR spectra, were employed in our studies with positively or negatively charged micellar solutions, respectively.<sup>46,47</sup>

The results (e.g., Figures 5 d1 and 5 d2) demonstrate that for a hydrophobic radical pair, the observed values of effective ESE

(45) Jenks, W. S.; Turro, N. J. *J. Am. Chem. Soc.* **1990**, *112*, 9009.

(46) Wang, J.; Welsh, K. M.; Waterman, K. C.; Fehlner, P.; Doubleday, C. J.; Turro, N. J. *J. Phys. Chem.* **1988**, *92*, 3730–3732.

(47) Molin, Y.; Salikhov, K.; Zamaraev, K. *Spin Exchange*; Springer-Verlag: New York, 1980; Chapter 4.

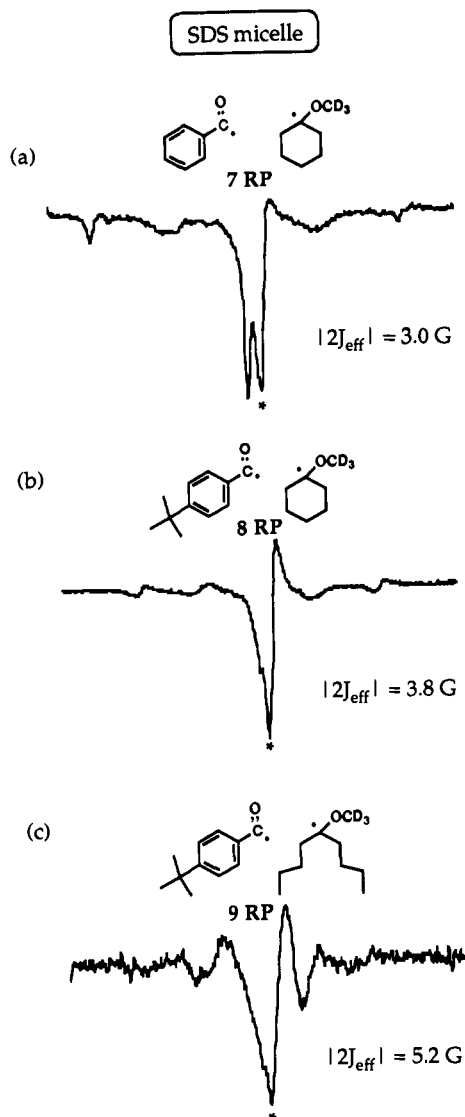


**Figure 4.** TRESR spectra obtained on photolysis of 7–9 K in SDS micellar solution. All spectra were recorded in the same conditions as those in Figure 3. The lines marked with asterisks are attributable to the benzoyl radicals; the remainder of the lines are attributable to the methoxy- $d_3$  radicals.

interaction ( $2J_{\text{eff}}$ ) are invariant in the TRESR spectra recorded both in the presence and in the absence of the added polarization quenchers, which means that the presence of the signals from the radical exiting the micelle has no significant interference on the observed values of  $2J_{\text{eff}}$  within the detection limit of 0.1 G. Nevertheless, the fast polarization quenching rates<sup>47,48</sup> of the aqueous paramagnetic quenchers can help evaluate the relative escape rates from micelles for the two geminate radical pair fragments, if at least one of the fragments is sufficiently hydrophilic. Escape of the individual fragments of a geminate radical pair is expected to be “anisotropic” and dependent on the hydrophobicities of the individual fragments. Figure 5 provides typical examples of how the relative escape rates of the micellized radical pair fragments are determined qualitatively by the polarization quencher located outside the micelle. All spectra are recorded at 450–500 ns after the photolysis of ketone molecules in DeTAB ( $C_{10}^+$ ) micellar solution. Two spectra for a series of radical pairs are presented, one in the absence and one in the presence of 5 mM  $Mn^{2+}$ .

Figure 5a shows that in the presence of 5 mM  $Mn^{2+}$ , the signal intensities of both polarized benzoyl and 2-propanoyl radicals

**Table I.** Number of Carbon Atoms Versus  $|J_{\text{eff}}|$  Values for the Radical Pairs in the SDS Micelle

common radical (no. of C atoms)	variable radical	no. of C atoms in variable radical	$ J_{\text{eff}} $ (G)
		3	$\sim 0$
		6	<1.2
		9	1.9
		7	1.5
		3	$\sim 0$
		6	1.6
		9	2.1
		7	1.9
		10	2.6

decrease but the intensity of the latter drops to a larger extent, indicating that the 2-propanoyl radical escapes faster from the DeTAB micelle than does the benzoyl radical. The difference in the ratio of radical escape rates can be amplified by increasing the hydrophobicity of the benzoyl radical, as shown in Figure 5b. In this case, a highly hydrophobic benzoyl radical is essentially “unquenched” by the  $Mn^{2+}$ , indicating that the polarized radical does not leave the micelle supercage during the time of observation. As a demonstration of the control of structure on the escape rates, the relative ratio of escape rates was reversed, i.e., the escape rate of a benzoyl radical was made to be faster than that of a more hydrophobic ketyl radical. Figure 5c shows such a reversal in the relative magnitude of the escape rates between the ketyl and benzoyl radicals by increasing the hydrophobicity of the ketyl-containing radical. Finally, the structure of both partners in the pair can be made sufficiently hydrophobic that neither partner escapes the micelle supercage during the time period of observation by TRESR. For example, when both radical pair fragments are very hydrophobic, as shown in Figure 5d, no change in the relative intensities of the TRESR spectra is observed upon the addition of  $Mn^{2+}$  on the observation time scale (500 ns), which demonstrates the relatively slow escape rates of both radicals. Thus, a comparison of the relative intensities in the presence and absence of quencher allows one to determine qualitatively the relative escape rates of the individual radical fragments from the micelle.

The effect of micelle size on polarization quenching of a given radical pair is revealed by comparing Figure 5c with Figure 5e. An increase in the detergent chain length from DeTAB ( $C_{10}^+$ ) to CTAB ( $C_{16}^+$ ) results in a complete elimination of polarization quenching by  $Mn^{2+}$ . In this case, the “effective” hydrophobicity of a given radical pair is increased by being associated with a

(48) Banci, L.; Bertini, I.; Luchinat, C. *Nuclear and Electron Relaxation*; VCH Publishers: New York, 1991; Chapter 5.

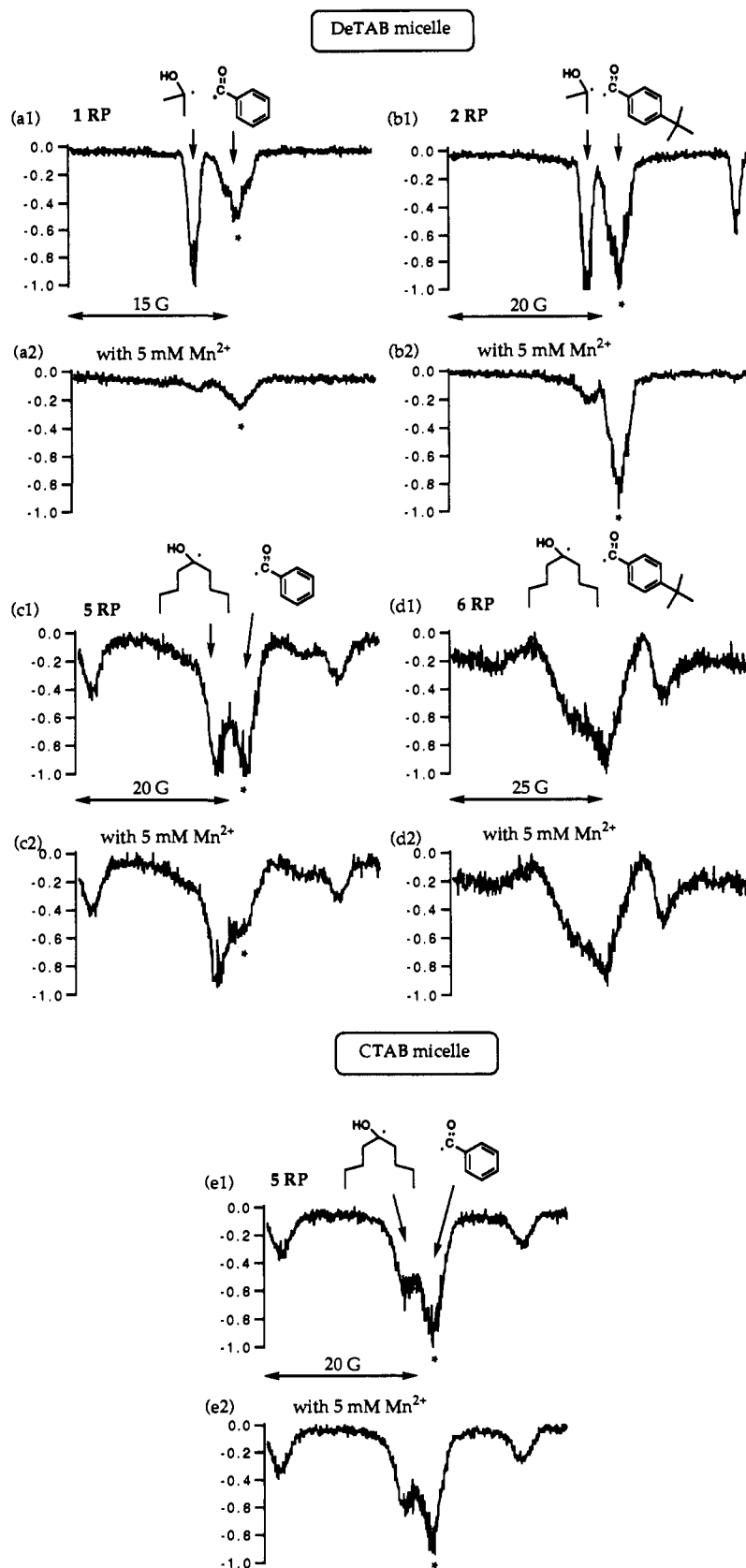


**Figure 5.** TRESR spectra obtained from photolysis of (a) 1 K, (b) 2 K, (c) 5 K, and (d) 6 K in DeTAB ( $C_{10}$ ) and (e) 5 K in CTAB ( $C_{16}$ ) micellar solutions. The effect of polarization quencher is studied by photolyzing each micellized ketone in the presence and absence of 5 mM  $Mn^{2+}$ . All spectra were recorded at 450–500 ns after the laser flash. The sweep width is 30 G for a, 40 G for b, c, and e, and 50 G for d. The lines attributable to the benzoyl radicals are marked with asterisks, while the rest of the lines are attributable to the ketyl radicals. For d, the lines are indistinguishable due to the strong correlation between the radical pair fragments.

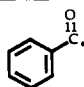
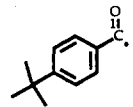
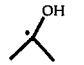
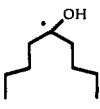
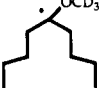
more hydrophobic micelle, again demonstrating the supramolecular characteristics of the micellized radical pair.

**Simulation of the TRESR Spectra.** The method employed for

simulation of the experimental TRESR spectra is based on the model described earlier by G. L. Closs and M. D. E. Forbes.<sup>12</sup> The basic assumptions of the model are the following.



**Table II.**  $g$  Values and Absolute Values of the Hyperfine Splitting Constants of the Radicals Used in the Spectra

simulation			
radical	$g$ value <sup>a</sup>	$A_{ortho}$ (G)	$A_{meta}$ (G)
	2.0008	0.21	1.18
	2.0008	0.21	1.18
radical	$g$ value <sup>b</sup>	$A(\beta\text{-CH}_2)$ (G) <sup>c</sup>	
	2.0033	20	
	2.0033	14.3–16.6*	
	2.0031	15.1–15.3*	

<sup>a</sup> (a) Bennett, J. E. *Trans. Faraday Soc.* **1971**, *67*, 1587. (b) Paul, H. *Helv. Chim. Acta* **1973**, 1575. <sup>b</sup> Berndt, A.; Fisher, H.; Paul, H. *Numerical Data and Functional Relationships in Science and Technology, Group II: Atomic and Molecular Physics, Vol. 9. Magnetic Properties of Free Radicals, Part b*; Fisher, H.; Hellwege, K.-H., Eds.; Springer-Verlag: Berlin, 1977. <sup>c</sup> The asterisk corresponds to values that depend on the environment (detergent chain length, salt concentration).

1. The magnetic properties of the micellized radical pair are treated in the high-field approximation, in which it is assumed that hyperfine interaction mixes only S and  $T_0$  states. This approximation is valid if the exchange interaction of radical sites is much less than the Zeeman splitting.

2. The rate of hyperfine-induced S– $T_0$  mixing within the radical pair is assumed to be fast relative to the decay rates. This assumption is made to keep the kinetic states tractable.

3. The effective exchange interaction is time-independent, i.e.,  $J_{eff} = \text{constant}$ . This assumption is required to make the calculation feasible but considered to be accepted as a “zero-order” approximation. The physical implication of this approximation is that the site equilibrium of radical pairs within the micelle has occurred before the initial observation has been made and that equilibrium is maintained during the recording of the TRESR spectra.

The details of the simulation program have been reported.<sup>12,18</sup> We followed the same basic approach to calculate the energy and intensity of each transition of the TRESR spectra. One minor modification was made in calculating the intensity, in which we employed linear combinations of the S and  $T_0$  states as the density matrix elements  $\rho$  of the two states after HFI-induced S– $T_0$  mixing. This modification is presented in detail in the Appendix.

The values of  $g$  factors and nuclear hyperfine coupling constants for the simulations were taken from the literature for radicals of identical or closely approximate structure to those investigated in this report (Table II). However, for 3 RP, 4 RP, 7 RP, and 8 RP, the hyperfine coupling constants of cyclohexyl protons are not well-defined on the time scale corresponding to the gate width of the boxcar due to the rapid ring flip in the cyclohexyl group.<sup>49–51</sup> Therefore, we have focused on the simulation of TRESR spectra involving 1, 2, 5, 6 RP, and 9 RP in various micellar environments.

(49) McLauchlan, K. A.; Stevens, D. G. *J. Chem. Phys.* **1987**, *87*, 4399.

(50) Corvaja, C.; Giacometti, G.; Brustolon, M. *J. Phys. Chem.* **1972**, *82*, 272.

(51) Corvaja, C.; Giacometti, G.; Sartori, G. *J. Chem. Soc., Faraday Trans.* **1974**, *70*, 709.

**Table III.** Effect of Radical Pair Structures on  $J_{eff}$ 

starting ketone	micelle	$J_{eff}$ (spectra) (G)	$J_{eff}$ (simulation) (G)	line width (G)
1	SDS (C <sub>12</sub> <sup>-</sup> )	~0	~0	0.8
2	SDS (C <sub>12</sub> <sup>-</sup> )	~0	~0	0.8
5	SDS (C <sub>12</sub> <sup>-</sup> )	-1.9	-1.8	3.0
6	SDS (C <sub>12</sub> <sup>-</sup> )	-2.1	-2.0	3.0
9	SDS (C <sub>12</sub> <sup>-</sup> )	-2.6	-2.7	4.5
6	CTAB (C <sub>16</sub> <sup>+</sup> )	-1.4	-1.4	1.0
9	CTAB (C <sub>16</sub> <sup>+</sup> )	-1.8	-1.8	2.5

The hyperfine coupling constants used for these five radical pairs are those of the ortho and meta protons for the benzoyl radicals and the  $\beta$ -alkyl protons in the dimethyl (from 1 and 2 RP) or dibutyl (from 5, 6, and 7 RP) radicals.

Variations of the recombination rates of geminate radical pairs,  $k_r$ , and of the exit rates of micellar radicals,  $k_e$ , were found to have a minor influence on the shape of the calculated spectra and only to affect the intensity of the spectra even when they are varied over 1 or 2 orders of magnitude. From data in the literature for similar micellar systems,<sup>21,27,52</sup> we set  $k_r$  equal to  $10^7$  s<sup>-1</sup> and  $k_e$  equal to  $10^6$  s<sup>-1</sup> for all simulation experiments.

The contribution of TM in the simulations can be controlled by changing the population of the initial triplet sublevels. In our computations, we increase the value of  $\rho_{11}(t)$  to make the initial  $T_+$  state overpopulated in comparison with the other two triplet sublevels, resulting in an entirely emissive spectrum. For a given radical pair precursor, the percentage of TM is kept constant in the entire series of experiments shown in Tables III–V.

As discussed above, a contribution from RPM can also be observed in all of the recorded TRESR spectra. The contribution of RPM increases with the time evolution of the recorded spectra (Figures 1b and 1c). We have used conventional procedures<sup>1,47,53,54</sup> to calculate the RPM ESR spectra of the selected radical pairs and introduced the final adjustment by multiplying the RPM ESR spectra by arbitrary coefficients and then adding them to the corresponding calculated ESR spectra of SCRP to obtain the best fit to the experimental TRESR spectra. The final simulated spectra were found to be most sensitive to the adjustable parameter  $J_{eff}$ . This parameter was varied to obtain the best fits as judged by a visual comparison and the results from these fits are shown in Tables III–V. The simulated spectra for micellized radical pairs derived from 1, 2, 5, 6 K, and 9 K at a given time (450–500 ns) are compared with the corresponding experimental TRESR spectra in Figure 6, and a reasonably good match in the position of the observed transitions is seen for all cases. However, the relatively shorter  $T_1$  relaxation time of the benzoyl radicals<sup>48</sup> is not taken into account in the spectral simulation; as a result, relatively higher intensities of the benzoyl radicals are observed, as expected, in all the simulation spectra.

A general result from Tables III–V is that all  $J_{eff}$  values are negative, which is consistent with the fact that all the radical pairs have been previously assigned singlet ground states. The magnitude of  $J_{eff}$  from the simulation is consistent with the values directly measured from the experimental spectra. Table III shows that  $J_{eff}$  decreases as the qualitative hydrophobicities (the number of carbon atoms in a radical fragment) of the radical pair structures decrease. Manipulating the micelle size by changing the detergent alkyl chain length (Table IV) or by adding electrolytes (Table V) shows that as the micelle size increases, the value of  $J_{eff}$  decreases. As mentioned earlier, for a given radical pair, the value of  $J$  is generally assumed to decrease exponentially with increasing radical pair separation. Therefore, the effective radical pair separation, which corresponds to  $L_{eff}$  within the detection time, is determined not only by the micelle size but also by the

(52) Scaiano, J. C.; Abuin, E. B.; Stewart, L. C. *J. Am. Chem. Soc.* **1982**, *104*, 5673.

(53) Pedersen, J. B.; Freed, J. H. *J. Chem. Phys.* **1973**, *58*, 2746.

(54) Pedersen, J. B.; Freed, J. H. *J. Chem. Phys.* **1973**, *59*, 2869.

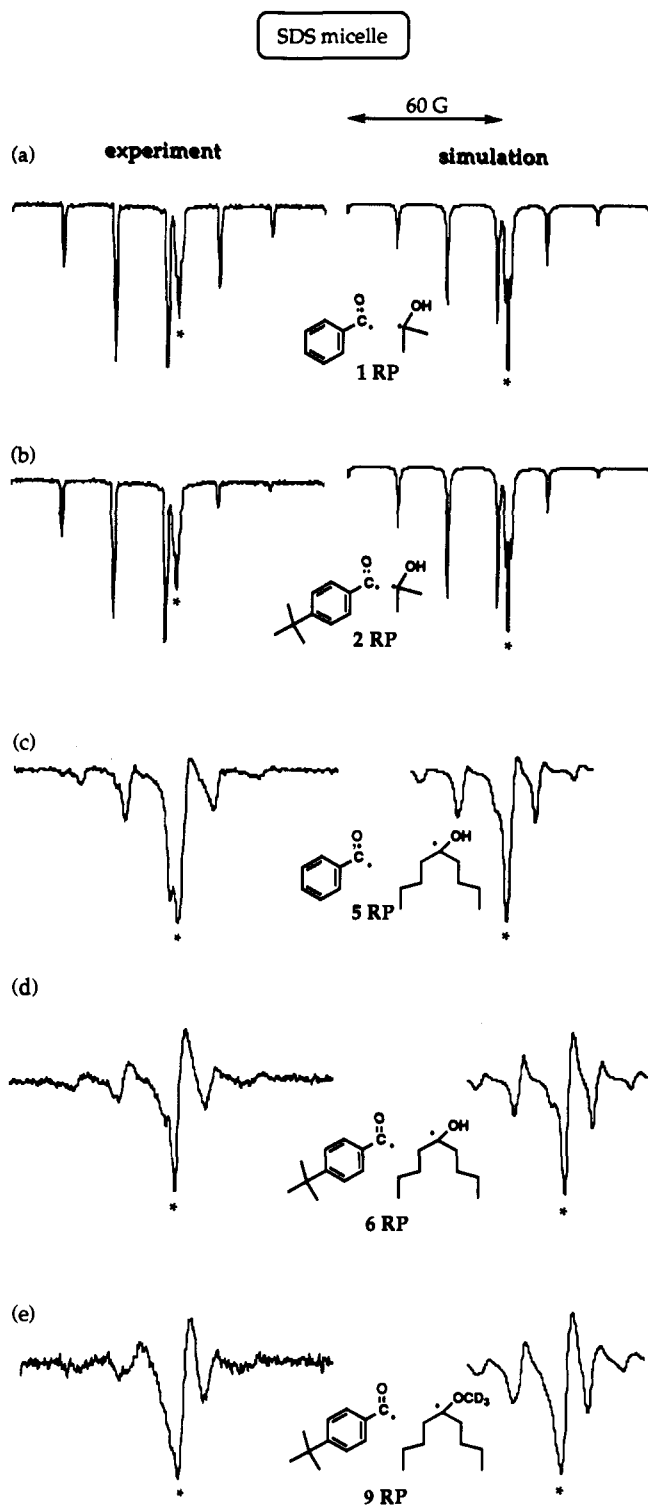


**Figure 6.** Simulation of the TRESR spectra obtained in the same conditions as those in figures 3 and 4. a–e correspond to photolysis of 1, 2, 5, 6 K, and 9 K in SDS micellar solution, respectively. All the signals attributable to the benzoyl radicals are marked with asterisks. The values of  $|2J_{\text{eff}}|$  derived from both experimental and simulation spectra are listed in Table III.

**hydrophobicities of the radical pairs.** This result emphasizes that the hydrophobicity of a micellized radical pair is a supramolecular property and therefore can be defined only by referring to the properties of both the micelle and the radical pair. With this supramolecular structural feature in mind, the influence of the radical pair structure on values of  $J_{\text{eff}}$  should be compared only for a given micelle. When this is done, the TRESR results for two radical pairs, which differ in only one of the radical fragments, may be compared and an estimate of the relative

**Table IV.** Effect of Detergent Chain Length on  $J_{\text{eff}}$

starting ketone	micelle	$J_{\text{eff}}$ (spectra) (G)	$J_{\text{eff}}$ (simulation) (G)	line width (G)
6	DeTAB ( $C_{10^+}$ )	-3.1	-3.1	3.5
6	DTAB ( $C_{12^+}$ )	-2.8	-2.5	2.5
6	TTAB ( $C_{14^+}$ )	-1.8	-1.8	2.0
6	CTAB ( $C_{16^+}$ )	-1.4	-1.4	1.0
6	SDeS ( $C_{10^-}$ )	-2.8	-2.8	3.5
6	SDS ( $C_{12^-}$ )	-2.0	-2.0	3.0

**Table V.** Effect of an Additive Electrolyte (NaCl) on  $J_{\text{eff}}$

starting ketone	micelle	[NaCl]	$J_{\text{eff}}$ (spectra) (G)	$J_{\text{eff}}$ (simulation) (G)	line width (G)
6	SDS ( $C_{12^-}$ )	0	-2.0	-2.0	3.0
6	SDS ( $C_{12^-}$ )	0.25	-1.7	-1.7	2.5
6	SDS ( $C_{12^-}$ )	0.5	-1.6	-1.6	2.0
6	SDS ( $C_{12^-}$ )	1.0	-1.2	-1.2	2.0

separation and the hydrophobicities of the noncommon fragments may be made.

The results of the spectral simulations are not as sensitive to the values of the line widths as they are to  $J_{\text{eff}}$  values. We estimate that this results in as much as 50% uncertainty to the best-fit value of the line width used. Nevertheless, Tables III and IV show that the tendency of the line width to increase with increasing hydrophobicities or with decreasing micelle size fits the qualitative picture. Interestingly, only a very small effect is seen on the line-width values when the salt concentration is changed (Table V).

## DISCUSSION

From the TRESR experiments, a value for the effective exchange interaction  $J_{\text{eff}}$  between spin-correlated radical pairs can be measured either directly from the spectra or through spectral simulation. To interpret properly and discuss the variation in  $J_{\text{eff}}$  as a function of micelle size and/or radical pair structure, we must take into account the diffusion dynamics of the pair inside the micelle as well as the spin evolution of the radical pairs under a negligible and under a finite exchange interaction and the fact that the instantaneous value of  $J$  is constantly modulated by the diffusion dynamics of the radical pair fragments.

In the following discussion, the micelle is modeled as a nonviscous homogeneous, spherical supercage or microreactor<sup>21,55</sup> with radius  $L$ , in which the radical pair fragments ACO and B possess a mutual diffusion coefficient  $D = D_1 + D_2$ , where  $D_1$  refers to the diffusion coefficient of ACO and  $D_2$  refers to the diffusion coefficient of B. In the model, we seek to connect the spatial separation  $r$  of the partners of the pair with the ability of the hyperfine coupling to induce intersystem crossing in the micellized radical pair. The physical assumption is that at certain small separations, the value of  $J$  will be sufficiently large to quench hyperfine-induced intersystem crossing but that at certain large separations, the value of  $J$  will be sufficiently small to allow hyperfine-induced intersystem crossing. If  $A_{\text{eff}}$  is the effective hyperfine interaction (HFI) experienced by the radical pair, then we can define a critical distance  $r^*$  as the separation between the paired radicals such that  $J(r^*) = A_{\text{eff}}$ . We now have a parameter to gauge when HFI-induced intersystem crossing (ISC) between nearly degenerate S and  $T_0$  states will be important. If the separation  $r$  between the paired radicals is greater than  $r^*$ , there is a near degeneracy of S and  $T_0$ ,  $J < A_{\text{eff}}$ , and intersystem crossing will be facile; however, if the separation  $r$  between the paired radicals is less than  $r^*$ ,  $J > A_{\text{eff}}$ , the near degeneracy between S and  $T_0$  is removed due to the strong exchange potential and ISC is inhibited. Thus,  $r^*$  is a useful distance parameter which can be compared to the micelle size and will determine the effective

role of HFI in the spin evolution of a given pair in micelles of different sizes.

We now address the method for evaluation of  $r^*$  for the micellar systems investigated. We start from eq 2, a conventionally accepted form for the distance dependence of exchange interaction<sup>47</sup> between two radicals with radii  $r_1$  and  $r_2$ .

$$J = J_0 \exp\left[\frac{-(r-R)}{\lambda}\right] \quad (2)$$

In eq 2,  $R = r_1 + r_2$  is the distance of closest approach of the radical pair and defines the "contact" state in which the pair is in the state of collision;  $\lambda$  is a parameter, whose value is usually assumed to be about  $0.5 \text{ \AA}$ ,<sup>56</sup> and a constant which determines the steepness with which the exchange interaction falls off as a function of radical pair separation;  $J_0$  is the value of the exchange interaction experienced in the contact state (i.e., radical pairs are in the state of collision) and is typically assumed to be about  $1.3 \times 10^{10} \text{ rad/s}$  for typical carbon radical pairs.<sup>21</sup>  $R$  is taken to be  $6 \times 10^{-8} \text{ cm}$  ( $6 \text{ \AA}$ ), which is a reasonable value for the radical pairs investigated. With an estimated value of  $A_{\text{eff}}$  ca.  $5.3 \times 10^8 \text{ rad/s}$  (30 G) or larger,<sup>57</sup> from eq 2, we compute that a typical value of  $r^* = 7.6 \times 10^{-8} \text{ cm}$  ( $7.6 \text{ \AA}$ ). The radius of micelles ( $L$ ) formed by sodium decyl sulfate ( $C_{10}^-$ ), the smallest sized detergent used in this study, is  $13 \times 10^{-8} \text{ cm}$  ( $13 \text{ \AA}$ )<sup>58,59</sup> which is still larger than the computed value of  $r^*$ . If  $Z$  is the frequency of encounters between the fragments of the micellized radical pair and  $D$  is the mutual diffusion coefficient inside the micelle, then  $Z = 3RD/(L^3 - R^3)$  and  $\tau = 1/Z$  is the time spent by the radical pair fragments separated from one another between encounters.<sup>24,42,60-62</sup> We can now define (eq 3) the critical parameter  $\tau^*$  as the time spent by the radical pair fragments between encounters within an imaginary sphere of radius  $r^*$ ,

$$\tau^* = \frac{L^3 - R^3}{3r^*D} \quad (3)$$

Since the micelle size is much larger than the size of the contact state ( $L^3 \gg R^3$ ), eq 4 provides a convenient approximation of  $\tau^*$ .

$$\tau^* = \frac{R}{r^*} \tau = \frac{L^3}{3r^*D} \quad (4)$$

Let us now consider two limiting cases which can be applied to the systems investigated: (1)  $A_{\text{eff}}\tau^* < 1$  and (2)  $A_{\text{eff}}\tau^* > 1$ . The physical implication of case 1 is the following: the micellized radical pair generally resides in a significant exchange potential, and hence, the probability of a transition between the  $T_0$  and S states, which are eigenfunctions of the exchange interaction, is very small. Thus, a triplet radical pair under case 1 has a small probability of undergoing intersystem crossing to a singlet, and the conditions for creating SCRPM (fast intersystem crossing to drain the  $T_0$  state) are not met. We term this a "static" case since the probability of ISC occurring between sequential encounters of the radical pair is very small. Assuming a homogeneous distribution of the radicals, integration of  $J$  through the distribution of the radical pair inside the micelle leads to the relation

(56) Bittl, R.; Schulten, K.; Turro, N. J. *J. Chem. Phys.* **1990**, *93*, 8260.

(57)  $A_{\text{eff}}^2 = \sum_i I_{ij}(I_{ij} + 1)A_{ij}^2$ . See: Steiner, U. E.; Ulrich, T. *Chem. Rev.* **1989**, *89*, 51.

(58) Tanford, C. *Physical Chemistry of Macromolecules* Wiley: New York, 1961; p40.

(59) Tanford, C. *J. Phys. Chem.* **1972**, *76*, 3020.

(60) Gosele, V.; Klein, U. K. A.; Hauser, M. *Chem. Phys. Lett.* **1979**, *68*, 291.

(61) Hatlee, M. D.; Kozak, J. J.; Rothenberger, G.; Infelta, P. D.; Gratzel, M. *J. Phys. Chem.* **1980**, *84*, 1508.

(62) Tachiya, M. In *Kinetics of Nonhomogeneous Processes. A Practical Introduction for Chemists, Biologists, Physicists and Material Scientists*; John Wiley: New York, 1987; p 575.

shown in eq 5. It is only in the static case that  $J_{\text{eff}} = \langle J \rangle_r$ .

$$J_{\text{eff}} = \langle J \rangle_r = \frac{J_0 \lambda R^2}{L^3} \quad (5)$$

For the systems investigated,  $A_{\text{eff}}$  is of the order of  $5.3 \times 10^8 \text{ rad/s}$  (30 G) or larger, a typical value of  $\tau^*$  is  $1.5 \times 10^{-8} \text{ s}$  when  $L$  is  $15 \times 10^{-8} \text{ cm}$  (e.g., the radius of an SDS micelle),  $r^* = 7.6 \times 10^{-8} \text{ cm}$ , and  $D = 1 \times 10^{-6} \text{ cm}^2/\text{s}$ . From eq 5 and these typical values, we compute that  $A_{\text{eff}}\tau^* = \text{ca. } 8$ , a value which makes case 1 ( $A_{\text{eff}}\tau^* < 1$ ) an unlikely condition for the systems investigated; therefore, we continue our discussion by assuming case 2 ( $A_{\text{eff}}\tau^* > 1$ ) is more appropriate for analysis of the micellized radical pairs studied.

The assumption that  $A_{\text{eff}}\tau^* > 1$  implies that there is sufficient time for spin evolution to occur between successive sets of encounters of the micellized radical pair. We term this the "dynamic" case. In this instance,  $J_{\text{eff}}$  can be defined by eq 6

$$J_{\text{eff}} = ZP_{\text{ex}} \quad (6)$$

where  $P_{\text{ex}}$  is the probability of an exchange event occurring per encounter.

The time spent by the radical pair in the contact state is given by  $R\lambda/D$  so that we may define a parameter,  $\mu$  (eq 7), where  $\mu$  is used to characterize  $P_{\text{ex}}$ .

$$\mu = \frac{R\lambda}{D} J_0 \quad (7)$$

When  $\mu > 1$ , the probability of exchange per encounter  $P_{\text{ex}} \rightarrow 1$ . From the assumed values of  $R = 6 \times 10^{-8} \text{ cm}$ ,  $\lambda = 5 \times 10^{-9} \text{ cm}$ ,  $J_0$  for micellized radical pairs =  $1.3 \times 10^{10} \text{ rad/s}$ , and  $D = 1 \times 10^{-6} \text{ cm}^2/\text{s}$  for diffusion coefficient in micelles, an estimate of  $\mu \approx 4$  is evaluated, which implies that  $P_{\text{ex}}$  is comparable to 1.

Since  $P_{\text{ex}}$  is ca. 1, the effective exchange interaction  $J_{\text{eff}}$  is given by eq 8.

$$J_{\text{eff}} = P_{\text{ex}}Z \approx Z = 3RD/L_3 \quad (8)$$

Thus, assuming a typical micellar radius of  $\sim 15 \times 10^{-8} \text{ cm}$  (15  $\text{\AA}$ ) and  $D = 1 \times 10^{-6} \text{ cm}^2/\text{s}$  for SDS micelles, we compute the rate of reencounter  $Z = 5.3 \times 10^7 \text{ s}^{-1}$  and  $2J_{\text{eff}} = 16.8 \text{ MHz}$  (6.0 G). This value is in reasonable agreement with the experimental values (see tables and figures), especially considering the extremely simple ideas involved in its estimation. Equation 8 also allows us to predict the influence of the micelle size on the value of  $J_{\text{eff}}$ . In an earlier study on alkyl sulfate micelles, it has been shown that  $D \propto L$ .<sup>21</sup> From eq 8, this result implies that  $Z \propto L^{-2}$  and hence  $J_{\text{eff}} \propto L^{-2}$ . For any given radical pair, the results show a clear decrease in the effective exchange interaction as the micelle size increases (Tables IV and V). This qualitative agreement supports our conclusion made at this level of sophistication. Closs et al. have found that upon photolysis of benzophenone- $d_{10}$  in sodium alkyl sulfate micelles, the magnitude of  $|2J_{\text{eff}}|$  decreases from 10.6 MHz (3.8 G) in  $C_{10}^-$  to 6.8 MHz (2.4 G) in  $C_{12}^-$  and then to 4.4 MHz (1.6 G) in  $C_{14}^-$ .<sup>12</sup> A similar trend of a decrease in  $J_{\text{eff}}$  was also observed when increasing the concentration of NaCl from 0.25 to 1.0 M in SDS micellar solution.<sup>12</sup>

Assuming  $A_{\text{eff}}\tau^* > 1$  and a high probability of exchange per encounter, we now attempt to rationalize the influence of the radical pair structure on the experimental values of  $J_{\text{eff}}$ . From eq 8, the three parameters which determine  $Z$  and hence  $J_{\text{eff}}$  are  $L$ ,  $R$ , and  $D$ . Although  $L$  has been defined as the micellar radius, it should be emphasized that  $L$  in reality is the effective radius of the micelle experienced by the radical pair fragments. There is no sharp delineation between the organic and aqueous domain of a micellar solution; water molecules are believed to penetrate

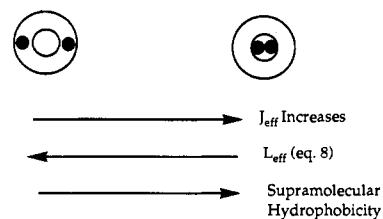
beyond the ionic head groups into the organic phase, and there may be a certain amount of monomer exchange with the aqueous phase during the TRESR measurements.<sup>40,63</sup> Thus, hydrophilic micellized radicals, such as those for which one of the partners possesses a ketyl group, may probe the micellar volume more completely than those radicals which contain strong hydrophobic substituents such as *tert*-butyl groups. From another point of view, the more hydrophilic radical pairs may reside predominantly in the polar, interfacial outer palisade layer and be able to achieve larger average separations, whereas more hydrophobic radical pairs may reside predominantly in the nonpolar, hydrocarbon-like inner core which comprises a relatively small portion of the total micelle volume. In either case, for a given micelle, the effective radius  $L_{\text{eff}}$  is expected to be larger for more hydrophilic radicals.

Increasing the number of substituents of any type will lead to an increase in the size of the collision complex  $R$  since the size of the radical fragments in the complex will effectively increase. However, a straightforward correlation cannot be drawn concerning the effect of size on the factors determining intersystem crossing because of the possibility of anisotropic effects of the micelle host on the stereochemistry and dynamics of substituted pairs, i.e., these effects may be sensitive to the specific location of the substituent as well as to the degree of branching that it introduces into the molecule. These ambiguities are another result of the supramolecular features of micellized radical pairs. However, it may be reasonably assumed that increasing the effective radius of the radical pair will lead to a decrease in the diffusion coefficient as predicted by the Stokes–Einstein equation.<sup>64</sup>

Strictly speaking, the most reliable conclusion that may be drawn concerning  $J_{\text{eff}}$  upon increasing the size of the radical pair structure is that the factor  $RD/L_{\text{eff}}^3$  will decrease relative to the radical pair with which it is being compared. However, at this level of approximation, the change in  $R$  ( $= r_1 + r_2$ ) is compensated by a corresponding change in  $D$  ( $\propto R^{-1}$ ) so that changes in  $J_{\text{eff}} \approx Z \propto (L_{\text{eff}}^3 \eta)^{-1}$  may be attributable to changes in  $L_{\text{eff}}$ . Table I shows that as the individual radical pair fragments become more hydrophobic, the value of  $|J_{\text{eff}}|$  increases. This result is consistent with the qualitative picture that the more hydrophobic radical pair fragments should be solubilized deeper in the relatively limited volume of the hydrophobic interior of the micelle,<sup>65,66</sup> thereby reducing the  $L_{\text{eff}}$  experienced by the radical pair fragments and resulting in a larger  $|J_{\text{eff}}|$ . At this point, we feel that hydrophobicity (an intuitively obvious concept) cannot be quantified more accurately<sup>43,67</sup> and related to  $L_{\text{eff}}$  to gain a better quantitative sense for the influence of the radical pair structure on  $J_{\text{eff}}$ .

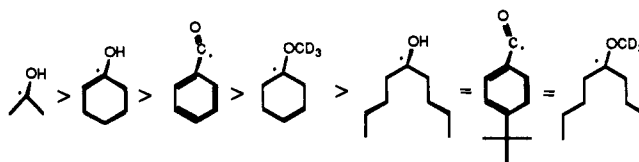
Some further conclusions concerning the dynamics of the radical pair escape from the micelle can be made from the polarization quenching experiments. By introducing paramagnetic quenchers to micellized radical pair systems, we were able to determine the relative escape rates of the micellized radical fragments in a given micelle. For the more hydrophobic micellized radical pairs like **6RP**, the intensities and patterns of the TRESR spectra observed are the same both in the presence and in the absence of polarization quenchers, implying slow escape rates from the micelles, and therefore, the observed spectra only contain signals from spin-correlated micellized radical pair fragments. Finally, from the results employing aqueous paramagnetic polarization quenchers, for the time scales of observation (up to 1.5  $\mu\text{s}$ ), the relative escape rates of radicals from a given micelle can be ranked. For example, a comparison of Figures 5 a1 and 5 a2 shows clearly

**Chart III.** Schematic Representation of the Influence of Supramolecular Hydrophobicity on the Values of  $J_{\text{eff}}$  and  $L_{\text{eff}}^a$



<sup>a</sup> The black circles represent the radicals and the inner circle represents the hydrophobic micellar core which is surrounded by the hydrophilic outer palisade layer.

that for benzoyl as a common radical of the pair, the dimethyl ketyl radical escapes much more rapidly than the dipentyl ketyl radical. Such comparisons allow, for a given micelle, the relative ranking of escape rates to be deduced.



It can be seen that the ranking is intuitively reasonable and, within a family of functional groups, the order scales simply as the number of hydrophobic carbon atoms in the radical.

## CONCLUSION

In summary, TRESR studies on the micellized radical pair system, a supramolecular system, provide a convenient method for measuring electron spin exchange interaction between the paramagnetic centers of the pair as a function of the molecular structure of the guest pair and of the size of the micelle host. On the basis of the spin-correlated radical pair model, we were able to compute the effective spin exchange interaction  $J_{\text{eff}}$  either from TRESR spectra of the given micellized radical pairs or through spectral simulation. Analysis of the results, employing a simple micellar model, indicates that the systems investigated are best classified as dynamic cases for which fast  $S-T_0$  intersystem crossing rates are induced by hyperfine interactions, i.e.,  $A_{\text{eff}}\tau^* > 1$ . In these cases, the values of  $J_{\text{eff}}$  are found to be most sensitive to the effective micelle size  $L_{\text{eff}}$  experienced by the micellized radical pairs.  $L_{\text{eff}}$ , besides obviously depending on the detergent chain length and added electrolyte (both affect the size of the micelle), is also a function of the radical pair structures. As the hydrophobic character of the micellized radical pair *supramolecular* system increases, the value of  $L_{\text{eff}}$  decreases and the value of  $J_{\text{eff}}$  increases (Chart III). The requirement to consider both the structure of a guest and a host in the interpretation of an observation is a signature characteristic of supramolecular systems.

**Acknowledgment.** The authors thank the National Science Foundation and the Air Force Office of Scientific Research for their generous support of this research.

## Appendix. Spectral Simulation of the TRESR Spectra via the SCRPM Model

The SCRPM proposed by Closs et al., which is the basis of the spectral simulation,<sup>12</sup> can be explained by the energy-level diagram of the micellized radical pair, as shown in Chart II. We have followed the same approach in spectral simulation as Closs did except for some minor modification in calculating the intensities of the ESR transitions. As shown in eq 9, the intensities of the ESR transitions  $\text{Int}_{nm}$  are given by the product of the transition

(63) Bolt, J. D.; Turro, N. J. *J. Phys. Chem.* **1981**, *85*, 4029.

(64) Connors, K. A. *Chemical Kinetics*; VCH Publishers: New York, 1990; p 135.

(65) Breslow, R. *Acc. Chem. Res.* **1991**, *24*, 159.

(66) Müller, N. *Acc. Chem. Res.* **1990**, *23*, 23.

(67) Hecht, D.; Tadesse, L.; Walters, L. *J. Am. Chem. Soc.* **1992**, *114*, 4336.

probabilities and the population differences between the states connected by the transition. The populations of the four transitions are given by the product of the density matrix elements with the corresponding rate factors.

$$\text{Int}_{12} = |\langle T_+ | S^+ | \Psi_2 \rangle|^2 [\rho_{22}(t)k_{22} - \rho_{11}(t)k_{11}] \quad (9a)$$

$$\text{Int}_{13} = |\langle T_+ | S^+ | \Psi_3 \rangle|^2 [\rho_{33}(t)k_{33} - \rho_{11}(t)k_{11}] \quad (9b)$$

$$\text{Int}_{24} = |\langle \Psi_2 | S^+ | T_- \rangle|^2 [\rho_{44}(t)k_{44} - \rho_{22}(t)k_{22}] \quad (9c)$$

$$\text{Int}_{34} = |\langle \Psi_3 | S^+ | T_- \rangle|^2 [\rho_{44}(t)k_{44} - \rho_{33}(t)k_{33}] \quad (9d)$$

In eq 9, both  $\Psi_2$  and  $\Psi_3$  are linearly combined wave functions of the electronic states  $T_0$  and  $S$  due to hyperfine-induced mixing,  $k_{nn}$  is the rate factor including the various growth and decay rate constants, and  $\rho_{nn}(t)$  is the time-dependent density matrix element. The solutions for  $\rho_{nn}(t)$  of the four electron pair states are listed in eq 10, based on the assumption that mixing is only for  $|T_0\rangle$  and  $|S\rangle$  and the initial condition of a triplet precursor without TM polarization.

$$\rho_{11}(t) = \rho_{44}(t) = 1/3 \quad (10a)$$

$$\rho_{22}(t) = \rho_{SS}(t)(\sin \theta)^2 + \rho_{T_0T_0}(t)(\cos \theta)^2 \quad (10b)$$

$$\rho_{33}(t) = \rho_{SS}(t)(\cos \theta)^2 + \rho_{T_0T_0}(t)(\sin \theta)^2 \quad (10c)$$

$$\rho_{SS}(t) = (1/3)(q^2 \sin^2 \omega t / \omega^2) \quad (11a)$$

$$\rho_{T_0T_0}(t) = (1/3)(1 - q^2 \sin^2 \omega t / \omega^2) \quad (11b)$$

In eq 10,  $\theta$  is dependent on  $J$  and the HFI, and  $\omega$  is from the stationary-state solutions for the wave functions resulting from  $S-T_0$  mixing and can be expressed as

$$\omega \cos 2\theta = J$$

Both programs use eigenfunctions  $\Psi_2$  and  $\Psi_3$  for transition matrix elements. For the density matrix elements, however, we used  $\rho_{22}(t)$  and  $\rho_{33}(t)$  from eigenfunctions  $\Psi_2$  and  $\Psi_3$  in our program, while in the original program,  $\rho_{SS}(t)$  and  $\rho_{T_0T_0}(t)$ , whose solutions are shown in eq 11, from the  $S$  and  $T_0$  states are used in the density matrix elements.<sup>12</sup>